International Journal of Automation and Computing, Volume 6, Number 1, February, 2009, Pages 14-21

Design of Poiseuille Flow Controllers Using the Method of Inequalities

John McKernan[1], James F Whidborne[2],
George Papadakis[1]

[1] Department of Mechanical Engineering, King's College London, Strand, London WC2R 2LS, UK
[2] Department of Aerospace Sciences, Cranfield University, Bedfordshire, MK43 0AL, UK

Abstract

This paper investigates the use of the Method of Inequalities (MoI) to design output-feedback compensators for the problem of the control of instabilities in a laminar plane Poiseuille flow. In common with many flows, the dynamics of streamwise vortices in plane Poiseuille flow are very non-normal. Consequently, small perturbations grow rapidly with a large transient that may trigger nonlinearities and lead to turbulence even though such perturbations would, in a linear flow model, eventually decay. Such a system can be described as a *conditionally linear system*. The sensitivity is measured using the maximum transient energy growth, which is widely used in the fluid dynamics community. The paper considers two approaches. In the first, the MoI is used to design low-order proportional and PI controllers. In the second approach, the MoI is combined with McFarlane and Glover's $\mathcal{H}_\infty$ loop-shaping design procedure in a mixed-optimization approach.

Keywords

Transient energy growth, transient behaviour, flow control, Poiseuille flow, Method of Inequalities (MoI), mixed optimization, $\mathcal{H}_\infty$-optimization.

1 Introduction

The problem of stabilizing fluid flows by feedback control has recently become a topic of much interest, e.g. [1]. Fluid flow dynamics are often highly non-normal — that is their eigenvectors are closely aligned — and this characteristic is one factor that makes fluid systems hard to control. Traditionally, fluid dynamicists have assessed the stability of systems using Lyapunov's first method, paying little attention to the eigenvectors and the system sensitivity. For non-normal flows this leads to difficulties in resolving the differences between measured and predicted flow instability [2]. Plane Poiseuille, or channel, flow is the unidirectional flow between two infinite parallel planes. This flow is laminar and stable for low Reynolds numbers, but at high Reynolds numbers the flow becomes unstable resulting in turbulence. Experiments show that the flow undergoes transition to turbulence for Reynolds number as low as 1000[3]. However, eigenvalue predictions show the flow to be stable at Reynolds numbers below approximately 5772 [4]. The non-normal nature of the dynamics makes the flow very sensitive. Hence an initial perturbation will grow to very large values before decaying. This can drive the system into regions where the non-linearities are significant and trigger turbulence.

The system dynamics can thus be considered as *conditionally linear*[5]. That is, the system can be considered linear provided the state remains within some region of the state space that is sufficiently close to the steady state. In this paper, we explicitly consider the energy of perturbations (or transient energy) which is a measure of the size of the perturbations of the state. It has a clear physical meaning and

is a fundamental notion in the study of turbulence and transition. Consequently, the maximum transient energy growth following some energy-bounded initial state perturbation is often used as a performance measure for fluid flow systems, e.g. [6, 7].

The problem of controlling plane Poiseuille flow has received considerable attention. For example, optimal linear quadratic methods have been considered by [7] and [8]. In these papers, the maximum transient energy growth is considered in the analysis of the design, but not explicitly in the design formulation. State feedback control that can minimize an upper bound on the maximum transient energy growth for plane Poiseuille flow is considered in [9]. However, state feedback is not available for fluid flow systems. The actual maximum transient energy growth can, in principle, be minimized for the output feedback problem[10], but the method is too computationally expensive for the Poiseuille flow problem. Furthermore it results in extremely high order controllers. Thus this paper considers two approaches that use the Method of Inequalities[11] (MoI). In the first, the MoI is used to design low-order controllers, namely proportional and PI controllers. In the second approach, the MoI is combined with McFarlane and Glover's $\mathcal{H}_\infty$ loop-shaping design procedure[12] in a mixed-optimization approach[13]. Preliminary results of the study can be found in [14].

A summary of the derivation of the state-space model is presented in the next section. This material can also be found in [9], but is reproduced here for convenience. A more detailed exposition can be found in [15], and full details in [16]. Section 3 defines the maximum transient energy growth and proposes that the control signal magnitude is measured in a similar way. The MoI and mixed optimization are introduced in Sections 4 and 5 respectively. The design results are given in Section 6. Finally, comments and conclusions are provided.

2 Plane Poiseuille flow

Incompressible fluid flow is described by the Navier-Stokes and continuity equations. The Navier-Stokes equations

$$\dot{\vec{U}} + \left(\vec{U} \cdot \nabla\right) \vec{U} = -\frac{1}{\rho}\nabla P + \frac{\mu}{\rho}\nabla^2 \vec{U} \tag{1}$$

form a set of three coupled, non-linear, partial differential equations representing Newton's second law where $\vec{U}$ is velocity, P is pressure, ρ is density (uniform) and μ is viscosity (uniform), and the continuity equation

$$\rho \nabla \cdot \vec{U} = 0 \tag{2}$$

is an additional constraint representing the conservation of mass.

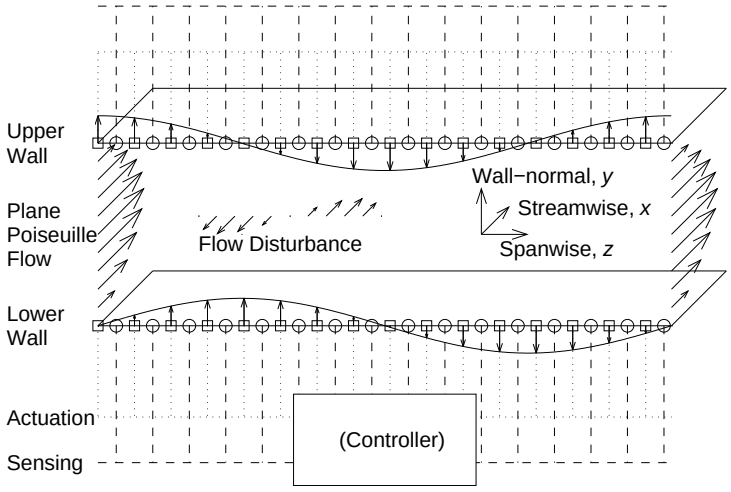

Figure 1: Plane Poiseuille flow.

The control scheme is illustrated in Fig. 1. This shows Laminar Poiseuille flow with no slip occurring at the bounding parallel planes, and which has a parabolic streamwise velocity profile. The flow undergoes transition to turbulence when small perturbations $\vec{u} = (u, v, w)$, p about the steady base profile, $\vec{U}_b = ((1-(y/h)^2)U_{cl}, 0, 0)$, P_b, grow spatially and temporally to form a self-sustaining turbulent flow.

The Navier-Stokes equations written in terms of perturbations about the base flow, $\vec{U}_b$, become

$$\dot{\vec{u}} + (\vec{u}\cdot\nabla)\,\vec{u} + \left(\vec{U}_b\cdot\nabla\right)\vec{u} + (\vec{u}\cdot\nabla)\,\vec{U}_b = -\frac{1}{\rho}\nabla p + \frac{\mu}{\rho}\nabla^2\vec{u} \tag{3}$$

If it is assumed that the perturbations are small compared to the base flow, the second-order nonlinear term, $(\vec{u}\cdot\nabla)\,\vec{u}$, can be discarded. Non-dimensionalizing (3) by dividing length scales by the channel half-height h, dividing velocities by the base centreline velocity U_{cl} and dividing pressure by ρU_{cl}^2, gives

$$\dot{\vec{u}} + \left(\vec{U}_b\cdot\nabla\right)\vec{u} + (\vec{u}\cdot\nabla)\,\vec{U}_b = -\nabla p + \frac{1}{R}\nabla^2\vec{u} \tag{4}$$

where $R := \rho U_{cl} h/\mu$ is the dimensionless Reynolds number. The continuity equation, (2), is linear and so becomes

$$\nabla\cdot\vec{u} = 0 \tag{5}$$

The state of the flow can be determined from wall shear-stress or pressure measurements, and the flow can be influenced by the manipulation of the conditions on its boundaries. In this work we assume that the shear-stress is measured and that the fluid is actuated by wall transpiration, which is the injection and suction of fluid at the walls. Hence active feedback control of the evolution of transition is feasible. The proposed feedback controller scheme is shown in Fig. 1. However, (4) and (5) are infinite dimensional, so in order to be able to use standard finite dimension control methods, and to ensure that the controller is practically implementable, they must be approximated by a finite dimension linear time-invariant system of the form

$$\begin{aligned}\dot{\mathbf{x}} &= \mathbf{A}\mathbf{x} + \mathbf{B}\mathbf{u}\\ \mathbf{y} &= \mathbf{C}\mathbf{x}\end{aligned} \tag{6}$$

However, a straightforward discretization results in a descriptor system with the form $\mathbf{E}\dot{\mathbf{x}} = \mathbf{A}\mathbf{x} + \mathbf{B}\mathbf{u}$ where $\mathbf{E}$ is singular. This is a consequence of the algebraic constraint imposed by the continuity equation, (5), that does not contain pressure.

To proceed, the pressure perturbation term is eliminated from (4) by substituting (5) giving an expression for the wall-normal velocity

$$\frac{\partial(\nabla^2 v)}{\partial t} + U_b\frac{\partial(\nabla^2 v)}{\partial x} - \frac{\partial^2 U_b}{\partial y^2}\frac{\partial v}{\partial x} - \frac{1}{R}\nabla^2(\nabla^2 v) = 0 \tag{7}$$

To completely describe a three dimensional flow perturbation, a second equation is required to describe the wall-normal vorticity, η, where

$$\eta = \frac{\partial u}{\partial z} - \frac{\partial w}{\partial x} \tag{8}$$

and (4) and (5) give

$$\frac{\partial \eta}{\partial t} + \frac{\partial U_b}{\partial y}\frac{\partial v}{\partial z} + U_b\frac{\partial \eta}{\partial x} - \frac{1}{R}\nabla^2\eta = 0 \tag{9}$$

To implement control by wall transpiration, the no-slip wall boundary conditions at $y = \pm 1$ are replaced by prescribed wall transpiration velocities, $(u(\pm 1) = 0, v(\pm 1) \neq 0, w(\pm 1) = 0)$. Sensing of $\partial u/\partial y$ and $\partial w/\partial y$ is performed at the upper and lower walls, as these are related to the streamwise and spanwise wall shear-stresses respectively. Disturbances on $\vec{u}$ vary in the streamwise (x), wall-normal (y), and spanwise (z) directions. Variations in the wall-normal direction are assumed to be non-periodic and are represented by a modified Chebyshev series that fulfils the wall boundary conditions [17]. Variations in the streamwise and spanwise directions are assumed to have a periodic representation, $\Re(e^{i(\alpha x+\beta z)})$, so flow disturbances grow in time, but not in space. The terms α and β are the streamwise and spanwise wave numbers

respectively. Substituting the assumed solutions into (7) and (9), and assuming an exponential time variation results in the classical Orr-Sommerfeld and Squire equations respectively[6].

After some manipulation of the equations, boundary control of the linearised Navier-Stokes equations in a channel at a particular wave number pair, (α, β) (with associated variables denoted by $\tilde{u}$, $\tilde{v}$, etc), can be represented as a linear state-space system in the standard form of (6). The linearised Navier-Stokes equations are evaluated at N locations in the wall-normal direction (with the locations more closely spaced near the walls), and the state variables $\mathbf{x}$ are the Chebyshev coefficients of the wall-normal velocity, $\tilde{v}$, and vorticity, $\tilde{\eta}$, perturbations concatenated with the upper and lower wall $\tilde{v}$ transpiration velocities. For details, see [16].

The inputs, $\mathbf{u}$, are the rates of change of upper and lower wall transpiration velocities. Since these are rates of change, the system contains two integrators, with eigenvectors representing upper and lower steady-state transpiration from the walls. The measurements, $\mathbf{y}$, are the wall shear-stress Fourier coefficients on the upper and lower walls. The Chebyshev coefficients are complex, but the state-space system is made real-valued by decomposing it into its real- and imaginary-valued parts, discarding the various null entries and thus leaving the state-space dimension the same size. The test case considered here is $\alpha = 0$, $\beta = 2.044$, $R = 5000$. This test case is linearly stable but has the largest transient energy growth over all unit initial conditions, time and wave-number pairs, and represents the very earliest stages of the transition to turbulence. The model is discretised in the wall-normal direction with $N = 20$. The order of the resulting model is $2N - 2$. A 38th order model is high for control purposes, but errors become significant at lower values of N [16].

3 Transient energy growth

Consider the asymptotically stable linear time-invariant system described by the initial value problem

$$\dot{\mathbf{x}} = \mathbf{A}\mathbf{x}, \quad \mathbf{x}(0) = \mathbf{x}_0, \tag{10}$$

with $\mathbf{A} \in \mathbb{R}^{n\times n}$, $\mathbf{x}_0 \in \mathbb{R}^n$ which has the continuous solution $\mathbf{x} : \mathbb{R}_+ \to \mathbb{R}^n$, $t \mapsto e^{\mathbf{A}t}\mathbf{x}_0$.

The transient energy, $\mathcal{E}(t)$, is defined as

$$\mathcal{E}(t) = \max\left\{ \|\mathbf{W}\mathbf{x}(t)\|^2 : \|\mathbf{W}\mathbf{x}(0)\| = 1 \right\}, \tag{11}$$

where $\mathbf{W} > 0$ is a constant weight matrix. The maximum transient energy growth, $\hat{\mathcal{E}}$, is defined as

$$\hat{\mathcal{E}} := \max\left\{ \mathcal{E}(t) : t \geq 0 \right\}. \tag{12}$$

Now consider the linear time-invariant plant

$$\begin{aligned} \dot{\mathbf{x}}(t) &= \mathbf{A}\mathbf{x}(t) + \mathbf{B}\mathbf{u}(t), \quad \mathbf{x}(0) = \mathbf{x}_0, \\ \mathbf{y}(t) &= \mathbf{C}\mathbf{x}(t), \end{aligned} \tag{13}$$

with $\mathbf{A} \in \mathbb{R}^{n\times n}$, $\mathbf{x}(t) \in \mathbb{R}^n$, $\mathbf{B} \in \mathbb{R}^{n\times \ell}$, $\mathbf{u}(t) \in \mathbb{R}^\ell$, $\mathbf{C} \in \mathbb{R}^{m\times n}$, $\mathbf{y}(t) \in \mathbb{R}^m$ with feedback controller

$$\begin{aligned} \dot{\mathbf{x}}_k(t) &= \mathbf{A}_k\mathbf{x}_k(t) + \mathbf{B}_k\mathbf{y}(t), \quad \mathbf{x}_k(0) = \mathbf{x}_{k0}, \\ \mathbf{u}(t) &= \mathbf{C}_k\mathbf{x}_k(t) + \mathbf{D}_k y(t), \end{aligned} \tag{14}$$

with $\mathbf{A}_k \in \mathbb{R}^{n_k\times n_k}$, $\mathbf{B}_k \in \mathbb{R}^{n_k\times m}$, $\mathbf{C}_k \in \mathbb{R}^{\ell\times n_k}$, $\mathbf{D}_k \in \mathbb{R}^{\ell\times m}$. The closed loop system is given by

$$\dot{\mathbf{x}}_c(t) = \mathbf{A}_c\mathbf{x}_c(t), \quad \mathbf{x}_c(0) = \mathbf{x}_{c0} \tag{15}$$

where

$$\mathbf{A}_c := \begin{bmatrix} \mathbf{A} + \mathbf{B}\mathbf{D}_k\mathbf{C} & \mathbf{B}\mathbf{C}_k \\ \mathbf{B}_k\mathbf{C} & \mathbf{A}_k \end{bmatrix}, \quad \mathbf{x}_c(t) := \begin{bmatrix} \mathbf{x}(t) \\ \mathbf{x}_k(t) \end{bmatrix}. \tag{16}$$

The maximum transient energy growth of the plant is

$$\hat{\mathcal{E}} = \max\left\{\|\mathbf{W}\mathbf{x}(t)\|^2 : \|\mathbf{W}\mathbf{x}_0\| = 1,\, \mathbf{x}_{k0} = 0,\, t \geq 0\right\}. \tag{17}$$

The transient energy in the controller states is irrelevant to the problem under consideration because the controller can always be normalized by appropriate choice of controller state basis. This is the problem of controller state scaling, see [18] for example. Further details about transient energy growth in finite dimension linear systems can be found in [10].

In order to limit the amount of effort generated by the controller in a closed loop system, the maximum control "transient energy growth" is defined as

$$\hat{\mathcal{U}} := \max\left\{\|\mathbf{u}(t)\|^2 : \|\mathbf{W}\mathbf{x}_0\| = 1,\, \mathbf{x}_{k0} = 0,\, t \geq 0\right\}, \tag{18}$$

where $\mathbf{u} = [\mathbf{D}_k\mathbf{C} \;\; \mathbf{C}_k]\mathbf{x}_c$.

4 The Method of Inequalities (MoI)

In the MoI [11], the control design problem is expressed as a set of algebraic inequalities that need to be satisfied for a successful design. The design problem is expressed as

$$\phi_i(\mathbf{p}) \leq \epsilon_i \text{ for } i = 1 \ldots n, \tag{19}$$

where ϵ_i are real numbers, $\mathbf{p} \in \mathcal{P}$ is a real vector $(p_1, p_2, \ldots, p_q)$ chosen from a given set $\mathcal{P}$ and ϕ_i are real functions of $\mathbf{p}$. The design goals ϵ_i are chosen by the designer and represent the largest tolerable values of the objective functions ϕ_i. The aim of the design is to find a $\mathbf{p}$ that simultaneously satisfies the set of inequalities.

A solution to the set of inequalities, (19), is obtained by means of numerical search algorithms. Generally, the design process is interactive, with the computer providing information to the designer about conflicting design requirements, and the designer adjusting the inequalities to explore the various possible solutions to the problem. The progress of the search algorithm should be monitored, and, if a solution is not found, the designer may either change the starting point, relax some of the design goals ϵ or change the design configuration. Alternatively, if a solution is found easily, to improve the quality of the design, the design goals could be tightened or additional design objectives could be included in (19). The design process is thus a two way process. The MoI provides information to the designer about conflicting design requirements, and the designer makes decisions about the 'trade-offs' between design requirements. Further details on numerical algorithms can be found in [11, 19, 20, 21].

The functions $\phi_i(\mathbf{p})$ are typically functionals of the system step response, for example the rise-time, overshoot or the integral absolute error, or functionals of the frequency response, such as the bandwidth. For the Poiseuille flow control problem they are taken as the maximum transient energy growth and the maximum control transient energy growth. To ensure these are finite, the system must be closed-loop stable and so a measure of the system stability needs to be included. One suitable measure is the maximum real part of the closed-loop eigenvalues

$$\alpha_0 = \max_i \{\Re(\lambda_i(\mathbf{A}_c))\} \tag{20}$$

where $\{\lambda_i\}$ represents the set of eigenvalues of the closed-loop system matrix, $\mathbf{A}_c$. Generally, the design parameter, $\mathbf{p}$, parameterizes a controller with a particular structure (e.g. [22]) rather than the state space structure of (14). For example, $\mathbf{p} = (p_1, p_2)$ could parameterize a P+I controller $p_1 + p_2/s$. Because state space realizations are over-parameterized, this ensures a smaller dimension of the search space, $\mathcal{P}$.

The Poiseuille flow control problem can be formulated as follows:

Problem 1. *Find a $\mathbf{p} \in \mathcal{P}$ and hence a $K(p)$ such that*

$$\alpha_0(\mathbf{p}) \leq \epsilon_\alpha, \tag{21}$$

$$\hat{\mathcal{E}}(\mathbf{p}) \leq \epsilon_{\hat{\mathcal{E}}}, \tag{22}$$

$$\hat{\mathcal{U}}(\mathbf{p}) \leq \epsilon_{\hat{\mathcal{U}}}, \tag{23}$$

where ϵ_α, $\epsilon_{\hat{\mathcal{E}}}$, and $\epsilon_{\hat{\mathcal{U}}}$ are prescribed tolerable values of α_0, $\hat{\mathcal{E}}$, and $\hat{\mathcal{U}}$ respectively.

5 Mixed optimization

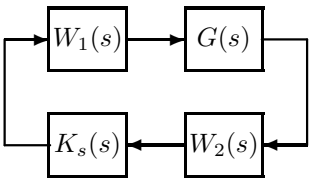

Figure 2: Controller configuration for LSDP

The MoI can be combined with analytical optimization techniques in a mixed optimization approach by using the parameters of the weighting functions generally required by such techniques as the design parameters [13, 23, 24]. Here, we use McFarlane and Glover's loop-shaping design procedure (LSDP) [12].

The LSDP maximizes robust stability to perturbations on the normalized coprime factors of a plant, $G(s)$, weighted by pre- and post-compensators $W_1(s)$ and $W_2(s)$ as shown in Fig. 2. An explicit controller $K(s)$ for optimal γ

$$\gamma_0 = \inf_K \left\| \begin{bmatrix} W_1^{-1}K \\ W_2 \end{bmatrix} (I - GK)^{-1} \begin{bmatrix} W_2^{-1} & GW_1 \end{bmatrix} \right\|_\infty \tag{24}$$

can be synthesized, the weights having been simply incorporated into the optimal controller $K_s(s)$ so that $K = W_1 K_s W_2$.

The problem can be formulated as the MoI as follows:

Problem 2. *For the system of Fig. 2, find a $\mathbf{p} \in \mathcal{P}$ and hence a $(W_1, W_2)(\mathbf{p})$ and K such that*

$$\gamma_0(\mathbf{p}) \leq \epsilon_\gamma, \tag{25}$$

$$\hat{\mathcal{E}}(\mathbf{p}) \leq \epsilon_{\hat{\mathcal{E}}}, \tag{26}$$

$$\hat{\mathcal{U}}(\mathbf{p}) \leq \epsilon_{\hat{\mathcal{U}}}, \tag{27}$$

where $(W_1, W_2)(\mathbf{p})$ is a pair of fixed order weighting functions with real parameters $\mathbf{p} = (p_1, p_2, \ldots, p_q)$ and ϵ_γ, $\epsilon_{\hat{\mathcal{E}}}$, and $\epsilon_{\hat{\mathcal{U}}}$ are prescribed tolerable values of γ_0, $\hat{\mathcal{E}}$, and $\hat{\mathcal{U}}$ respectively.

6 Results

6.1 Open loop

The transient energy $\mathcal{E}(t)$ of the linearized system with no wall transpiration control is shown in Fig. 3. The maximum transient energy growth is $\hat{\mathcal{E}} = 4941$.

6.2 Low order controllers

The design goals are set at

$$\epsilon_\alpha = -1 \times 10^{-5}, \tag{28}$$

$$\epsilon_{\hat{\mathcal{E}}} = 1000, \tag{29}$$

$$\epsilon_{\hat{\mathcal{U}}} = 1. \tag{30}$$

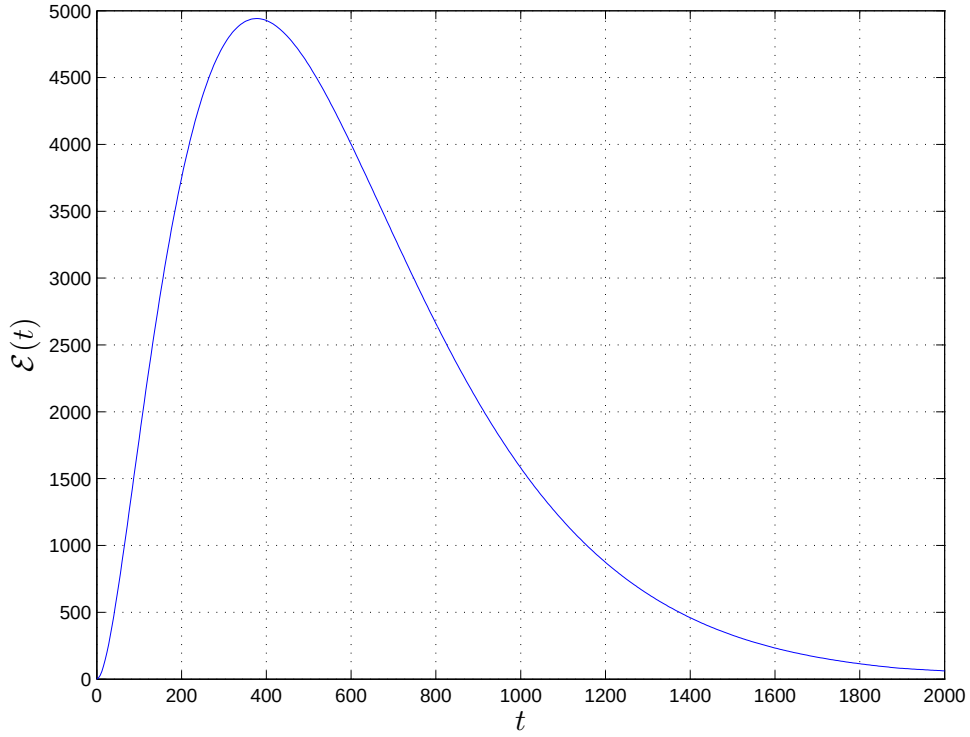

Figure 3: Transient energy for open-loop system.

As the control vector, $\mathbf{u}$, consists of the rates of change of upper and lower wall transpiration velocity, and the measurement vector, $\mathbf{y}$, consists of the upper and lower wall shear-stress, this symmetry can be exploited in the definition of the controller structure to halve the number of search parameters. Matching the symmetrical and the antisymmetrical input-output pairs gives a controller structure

$$K(s) := \begin{bmatrix} K_1(s) & K_2(s) & K_3(s) & K_4(s) \\ K_2(s) & K_1(s) & K_4(s) & K_3(s) \end{bmatrix}. \tag{31}$$

Several low-order structures were tried using the Moving Boundaries Process[11] (MBP), but no controller was found that satisfied Problem 1. After some iterations, the proportional controller

$$K = \begin{bmatrix} 0.9424 & 0.8562 & 0.2179 & 0.1022 \\ 0.8562 & 0.9424 & 0.1022 & 0.2179 \end{bmatrix} \tag{32}$$

was obtained with a performance

$$\alpha_0 = -1.7885 \times 10^{-3}, \tag{33}$$

$$\hat{\mathcal{E}} = 2740.0, \tag{34}$$

$$\hat{\mathcal{U}} = 0.9983. \tag{35}$$

The transient energy $\mathcal{E}(t)$ is shown in Fig. 4, and the control transient energy is shown in Fig. 5. Detail of the control transient energy is shown in Fig. 6.

In order to improve the performance, integral action was added by defining a PI structure for each $K_i(s)$, $i = 1, 2, 3, 4$ of (31) as

$$K_i(s) = k_i \left(1 + 1/sT_i\right). \tag{36}$$

A controller with

$$k = \begin{bmatrix} 0.7522 & 1.0184 & 0.4109 & 0.0292 \end{bmatrix} \tag{37}$$

$$T = \begin{bmatrix} 51.7557 & 65.3167 & 145.1924 & 18.5902 \end{bmatrix} \tag{38}$$

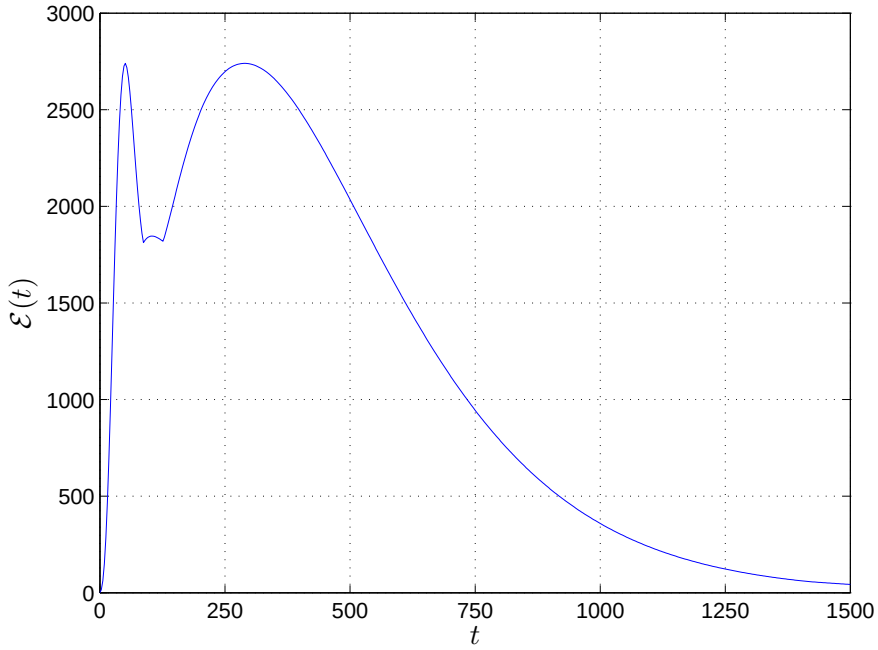

Figure 4: Transient energy for proportional controller.

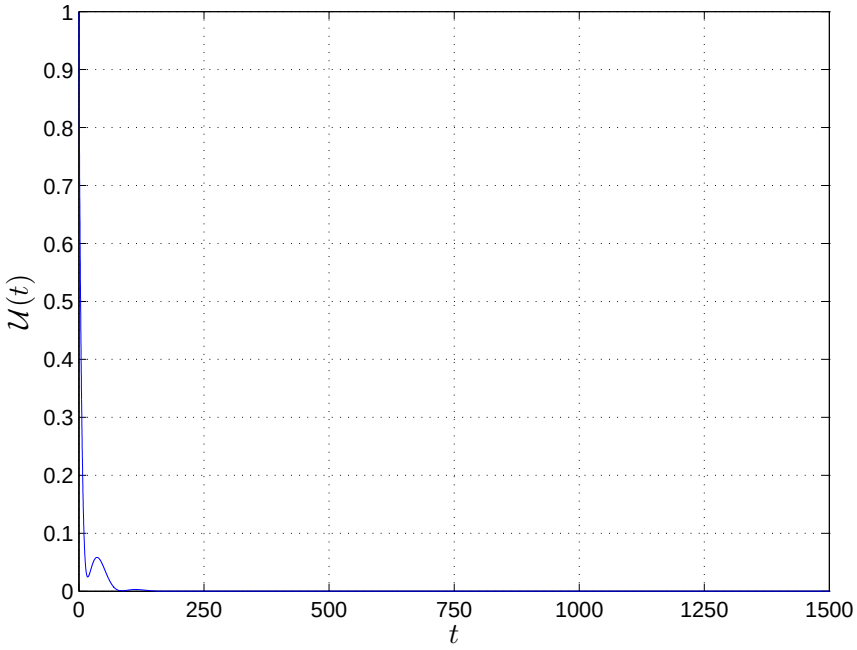

Figure 5: Control transient energy for proportional controller.

was found by the MBP with a performance

$$\alpha_0 = -1.7691 \times 10^{-3}, \tag{39}$$

$$\hat{\mathcal{E}} = 2690.5, \tag{40}$$

$$\hat{\mathcal{U}} = 0.9960, \tag{41}$$

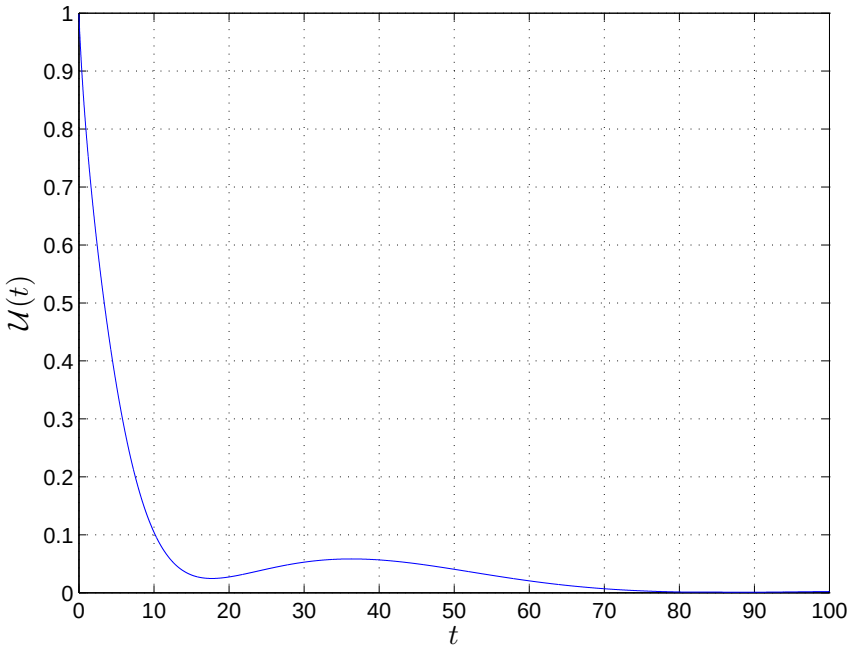

Figure 6: Control transient energy for proportional controller (detail).

which is an improvement on the proportional controller. The transient energy $\mathcal{E}(t)$ is shown in Fig. 7, and the control transient energy is shown in Fig. 9. Detail of the control transient energy is shown in Fig. 9.

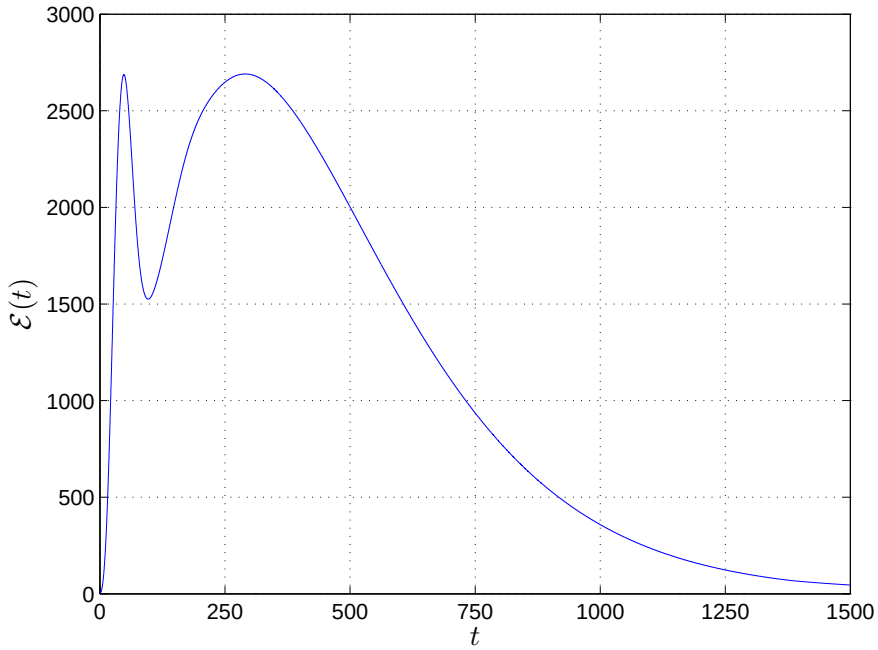

Figure 7: Transient energy for PI controller.

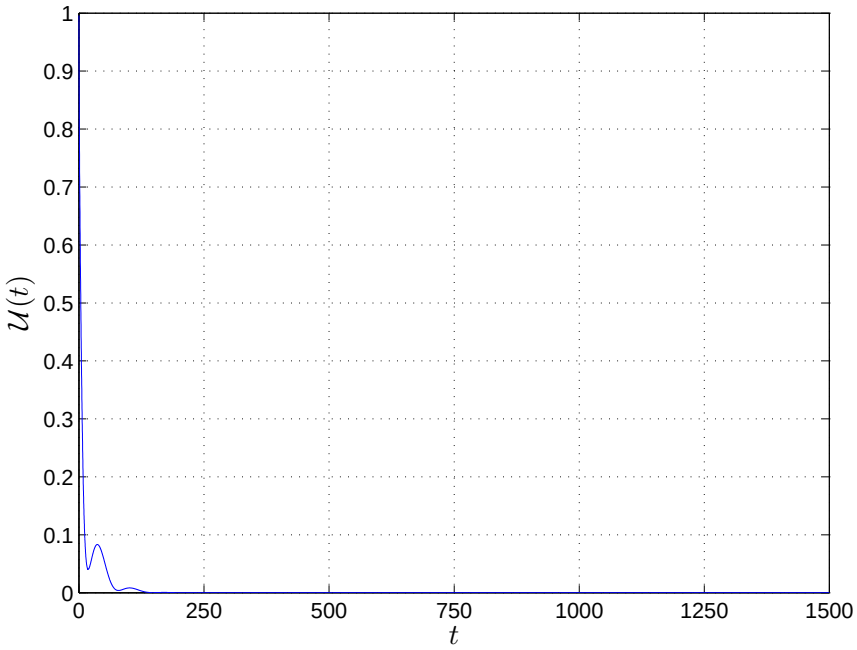

Figure 8: Control transient energy for PI controller.

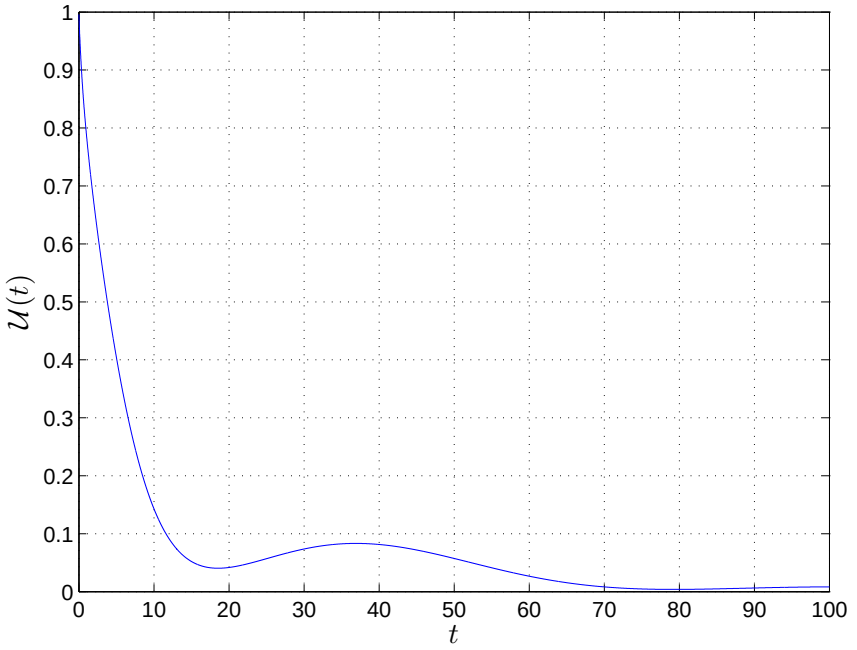

Figure 9: Control transient energy for PI controller (detail).

PD and a PID structures were also tried, but the addition of derivative action gave only a very small performance improvement with a very large increase in control effort. Some results for a PD controller are presented in [14].

6.3 Mixed optimization

The design goals are set for Problem 2 at

$$\epsilon_\gamma = 5, \tag{42}$$
$$\epsilon_{\hat{\mathcal{E}}} = 1000, \tag{43}$$
$$\epsilon_{\hat{\mathcal{U}}} = 10. \tag{44}$$

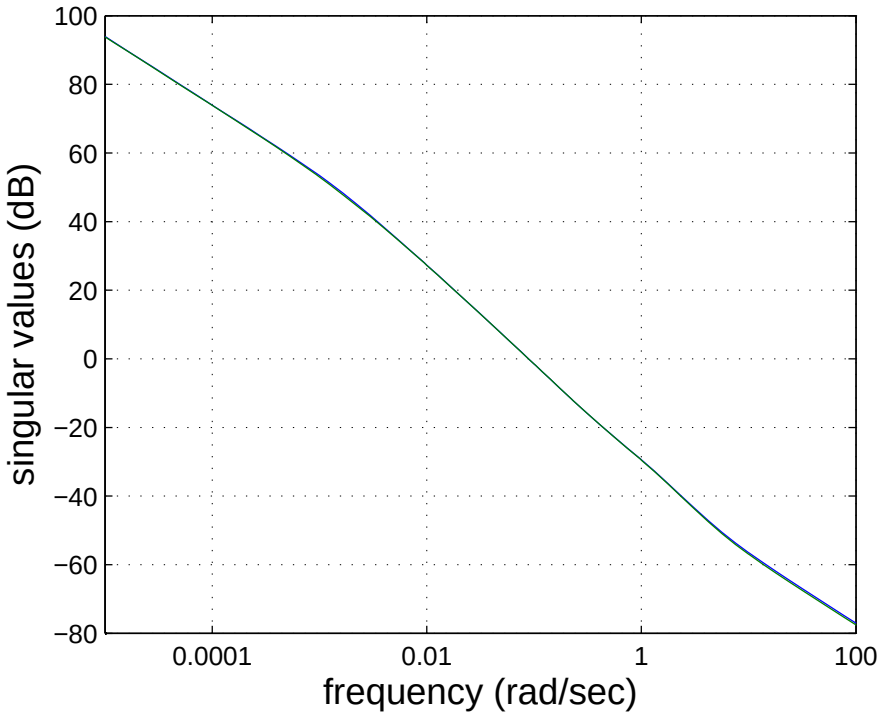

Figure 10: Open-loop singular values.

The open-loop singular values plot is shown in Fig. 10. The two singular value curves are very close. Hence diagonal weighting functions matrices were chosen with both diagonal terms equal, that is $W_1(s) = \text{diag}(w(s), w(s))$. The post-plant weighting was set to be the identity $W_2 = I$. Several structures for $w(s)$ were tried. The best performance was obtained with the structure

$$w(s) = \frac{p_1 s + p_2}{p_3 s + p_4} \tag{45}$$

and with

$$p = \begin{bmatrix} 0.7278 & 1.7784 & 0.7095 & 0.4631 \end{bmatrix}. \tag{46}$$

The design goal, $\epsilon_{\hat{\mathcal{E}}}$ was not satisfied. The resulting performance was

$$\gamma_0 = 2.0194, \tag{47}$$
$$\hat{\mathcal{E}} = 2874.0, \tag{48}$$
$$\hat{\mathcal{U}} = 0.9999. \tag{49}$$

The transient energy $\mathcal{E}(t)$ is shown in Fig. 11. Interestingly, the best value of $\hat{\mathcal{E}}$ was marginally greater than that for the proportional controller, but the $\mathcal{H}_\infty$-optimal controller prevented the possibility of an earlier energy growth, as seen by the absence of peaks in the transient energy curve for time less than 250. The control transient energy is shown in Fig. 12 and detail is shown in Fig. 13.

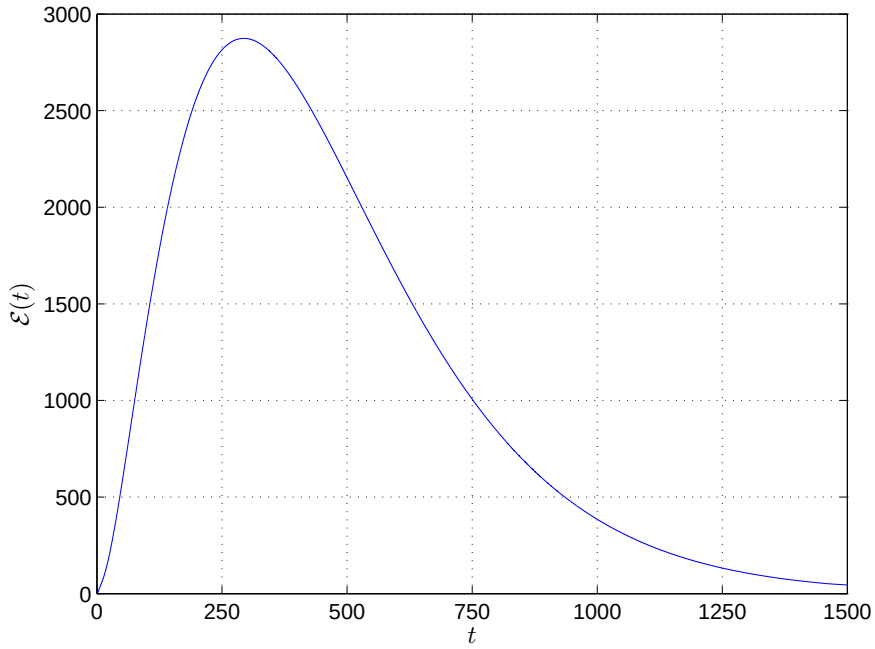

Figure 11: Transient energy for LSDP controller.

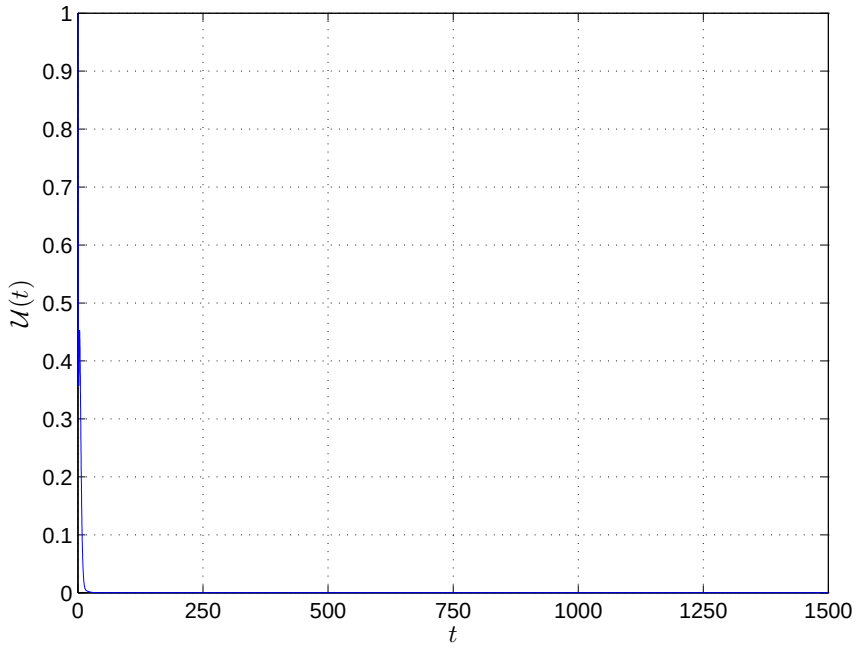

Figure 12: Control transient energy for LSDP controller.

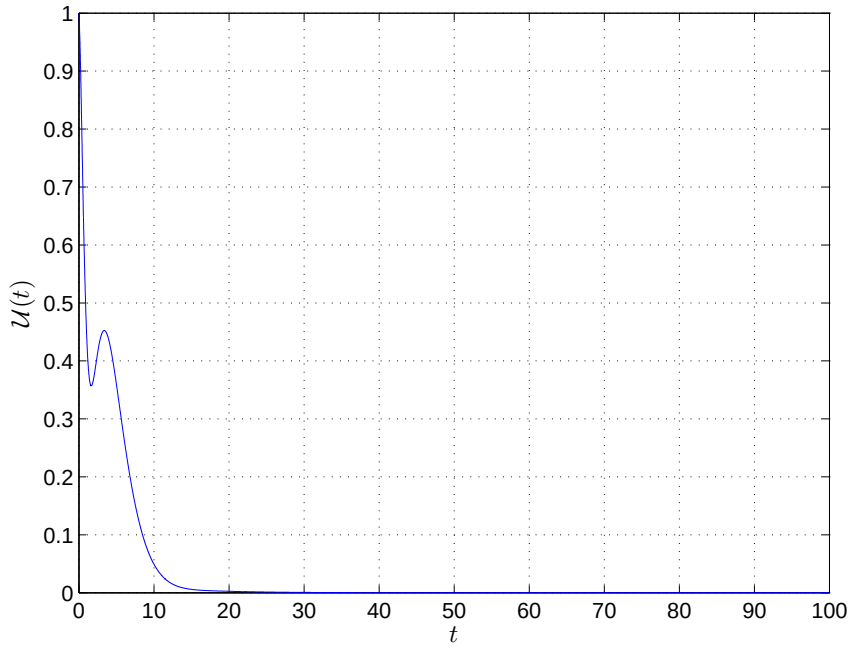

Figure 13: Control transient energy for LSDP controller (detail).

7 Discussion and conclusions

In this paper, the design of both low order controllers and $\mathcal{H}_\infty$-optimal controllers using the MoI has been performed. The state feedback controllers obtained in [9] gave a value of $\hat{\mathcal{E}} = 883$. This is considerably lower than the best value obtained in this study of $\hat{\mathcal{E}} = 2690.5$ for the PI controller. This indicates the difficulties in state estimation for this system. The optimal $\mathcal{H}_\infty$ was unable to improve on the PI controller and was actually greater. However, the performance of the transient energy was significantly better for earlier times. With an increase in computational power, the convex optimization methods of [10] could be applied to this problem and determine what is the minimal $\hat{\mathcal{E}}$ and whether a solution exists. The problem of model order reduction for the maximum transient energy growth problem would aid the design of optimal controllers, but that is a topic for further study.

Proportional control performed by [7] achieves a lower transient energy growth. However the model actuates by wall-normal velocity, rather than rate-of-change of wall-normal velocity. More recent work indicates that control by rate-of-change of velocity results in greater accuracy when modelling flow control for plane Poiseuille flow due to improved treatment of the Neumann boundary conditions and energy weighting matrix W [15, 8]. Note also that the design of low-order controllers for the problem of plane Poiseuille flow has been considered before [25] but but not the explicit consideration of the maximum transient energy growth. Similarly, McFarlane and Glover's LSDP has been used for a spatially growing channel flow [26], but transient energy growth was also not explicitly considered.

References

[1] S. Scott Collis, R.D. Joslin, A. Seifert, and V. Theofilis. Issues in active flow control: theory, control, simulation, and experiment. *Progress in Aerospace Sciences*, 40(4-5):237–289, 2004.

[2] J.S. Baggett, T.A. Driscoll, and L.N. Trefethen. A mostly linear model of transition to turbulence. *Physics of Fluids*, 7(4):833–838, 1995.

[3] D.R. Carlson, S.E. Widnall, and M.F. Peeters. A flow-visualization study of transition in plane Poiseuille flow. *J. Fluid Mech.*, 121:487–505, 1982.

[4] S.A. Orszag. Accurate solution of the Orr-Sommerfeld stability equation. *J. Fluid Mech.*, 50(4):689–703, 1971.

[5] V. Zakian. New formulation for the method of inequalities. *Proc. IEE*, 126(6):579–584, 1979. (reprinted in *Systems and Control Encyclopedia*, 1987, Pergamon Press, vol. 5, pp. 3206–3215).

[6] P.J. Schmid and D.S. Henningson. *Stability and Transition in Shear Flows*, volume 142 of *Applied Mathematical Sciences*. Springer, New York, 2001.

[7] T.R. Bewley and S. Liu. Optimal and robust control and estimation of linear paths to transition. *J. Fluid Mech.*, 365:305–349, 1998.

[8] J. McKernan, J.F. Whidborne, and G. Papadakis. Linear quadratic control of plane Poiseuille flow - the transient behaviour. *Int. J. Control*, 80(12):1912–1930, 2007.

[9] J.F. Whidborne, J. McKernan, and G. Papadakis. Minimising transient energy growth in plane poiseuille flow. *Proc. IMechE J. Syst. Contr. Eng.*, 222(5):323–331, 2008.

[10] J.F. Whidborne and J. McKernan. On minimizing maximum transient energy growth. *IEEE Trans. Autom. Control*, 52(9):1762–1767, September 2007.

[11] V. Zakian and U. Al-Naib. Design of dynamical and control systems by the method of inequalities. *Proc. IEE*, 120(11):1421–1427, 1973.

[12] D.C. McFarlane and K. Glover. *Robust Controller Design Using Normalized Coprime Factor Plant Descriptions*, volume 138 of *Lect. Notes Control & Inf. Sci.* Springer-Verlag, Berlin, 1990.

[13] J.F. Whidborne, I. Postlethwaite, and D.-W. Gu. Robust controller design using H_∞ loop-shaping and the method of inequalities. *IEEE Trans. Control Syst. Technology*, 2(4):455–461, 1994.

[14] J.F. Whidborne, J. McKernan, and G. Papadakis. Poiseuille flow controller design via the method of inequalities. In *Proc. UKACC Int. Conf. CONTROL 2008*, page CDROM paper 150, Manchester, U.K., September 2008.

[15] J. McKernan, G. Papadakis, and J.F. Whidborne. A linear state-space representation of plane Poiseuille flow for control design – a tutorial. *Int. J. Model. Ident. and Control*, 1(4):272–280, 2006.

[16] J. McKernan. *Control of Plane Poiseuille Flow: A Theoretical and Computational Investigation*. PhD thesis, Cranfield University, 2006.

[17] J. McKernan, G. Papadakis, and J.F. Whidborne. Linear and non-linear simulations of feedback control in plane Poiseuille flow. *Int. J. Numer. Methods Fluids*, 2008. Published online.

[18] M.E. Ahmed and P.R. Belanger. Scaling and roundoff in fixed-point implementation of control algorithms. *IEEE Trans. Ind. Electr.*, 31(3):228–234, 1984.

[19] J.F. Whidborne, D.-W. Gu, and I. Postlethwaite. Algorithms for the method of inequalities – a comparative study. In *Proc. 1995 Amer. Contr. Conf.*, pages 3393–3397, Seattle, WA, June 1995.

[20] C.M. Fonseca and P.J. Fleming. Multiobjective optimization and multiple constraint handling with evolutionary algorithms – part I: a unified formulation. *IEEE Trans. Syst. Man & Cybernetics – A*, 28(1):26–37, 1998.

[21] V. Zakian, editor. *Control Systems Design - A New Framework*. Springer, London, U.K., 2005.

[22] G.P. Liu, J.B. Yang, and J.F. Whidborne. *Multiobjective Optimisation and Control*. Research Studies Press, Baldock, UK, 2002.

[23] J.F. Whidborne, G. Murad, D.-W. Gu, and I. Postlethwaite. Robust control of an unknown plant – the IFAC 93 benchmark. *Int. J. Control*, 61(3):589–640, 1995.

[24] I. Postlethwaite, J.F. Whidborne, G. Murad, and D.-W. Gu. Robust control of the benchmark problem using H_∞ methods and numerical optimization techniques. *Automatica*, 30(4):615–619, 1994.

[25] S.S. Joshi, J.L. Speyer, and J. Kim. A systems theory approach to the feedback stabilization of infinitesimal and finite-amplitude disturbances in plane Poiseuille flow. *J. Fluid Mech.*, 332(4):157–184, 1997.

[26] L. Baramov, O.R. Tutty, and E. Rogers. $\mathcal{H}_\infty$ control of nonperiodic two-dimensional channel flow. *IEEE Trans. Control Syst. Technology*, 12(1):111–122, 2004.